A posteriori correction of DG schemes through subcell finite volume formulation and flux recontruction

François Vilar

Institut Montpelliérain Alexander Grothendieck
Université de Montpellier

17 Octobre 2019

1. Introduction
2. DG as a subcell finite volume
3. *A posteriori* subcell correction
4. Numerical results
5. Conclusion

History

- Introduced by Reed and Hill in 1973 in the frame of the neutron transport
- Major development and improvements by B. Cockburn and C.-W. Shu in a series of seminal papers

Procedure

- Local variational formulation
- Piecewise polynomial approximation of the solution in the cells
- Choice of the numerical fluxes
- Time integration

Advantages

- Natural extension of Finite Volume method
- Excellent analytical properties (L_2 stability, $hp-$adaptivity, ...)
- Extremely high accuracy (superconvergent for scalar conservation laws)
- Compact stencil (involve only face neighboring cells)

Scalar conservation law

- $\dfrac{\partial u}{\partial t} + \nabla \cdot \mathbf{F}(u) = 0, \qquad (\mathbf{x}, t) \in \omega \times [0, T]$
- $u(\mathbf{x}, 0) = u_0(\mathbf{x}), \qquad \mathbf{x} \in \omega$

$(k+1)^{\text{th}}$ order semi-discretization

- $\{\omega_c\}_c$ a partition of ω, such that $\omega = \bigcup_c \omega_c$
- $u_h(\mathbf{x}, t)$ the numerical solution, such that $u_{h|\omega_c} = u_h^c \in \mathbb{P}^k(\omega_c)$

$$u_h^c(\mathbf{x}, t) = \sum_{m=1}^{N_k} u_m^c(t)\, \sigma_m(\mathbf{x})$$

- $\{\sigma_m\}_{m=1,\dots,N_k}$ a basis of $\mathbb{P}^k(\omega_c)$, with $N_k = \frac{(k+1)(k+2)}{2}$ in 2D.

Local variational formulation on ω_c

- $\displaystyle\int_{\omega_c} \left(\frac{\partial u}{\partial t} + \nabla \cdot \mathbf{F}(u) \right) \psi \, \mathrm{d}V = 0$ with $\psi(\mathbf{x})$ a test function

Integration by parts

- $$\int_{\omega_c} \frac{\partial u}{\partial t}\psi \,\mathrm{d}V - \int_{\omega_c} \mathbf{F}(u)\,\boldsymbol{.}\,\nabla\psi \,\mathrm{d}V + \int_{\partial\omega_c} \psi\, \mathbf{F}(u)\,\boldsymbol{.}\,\mathbf{n}\,\mathrm{d}S = 0$$

Approximated solution

- Substitute u by u_h^c, and restrict ψ to the polynomial space $\mathbb{P}^k(\omega_c)$
- $$\int_{\omega_c} \frac{\partial u_h^c}{\partial t}\psi \,\mathrm{d}V = \int_{\omega_c} \mathbf{F}(u_h^c)\,\boldsymbol{.}\,\nabla\psi \,\mathrm{d}V - \int_{\partial\omega_c} \psi\, \mathcal{F}_n\,\mathrm{d}S, \qquad \forall\,\psi \in \mathbb{P}^k(\omega_c)$$
- $$\sum_{m=1}^{N_k} \frac{\mathrm{d}\,u_m^c}{\mathrm{d}t} \int_{\omega_c} \sigma_m\,\sigma_p \,\mathrm{d}V = \int_{\omega_c} \mathbf{F}(u_h^c)\,\boldsymbol{.}\,\nabla\sigma_p \,\mathrm{d}V - \int_{\partial\omega_c} \sigma_p\, \mathcal{F}_n\,\mathrm{d}S, \qquad \forall\,p \in [\![1, N_k]\!]$$

Numerical flux

- $\mathcal{F}_n = \mathcal{F}\left(u_h^c, u_h^v, \mathbf{n}\right)$
- $$\mathcal{F}(u, v, \mathbf{n}) = \frac{\left(\mathbf{F}(u) + \mathbf{F}(v)\right)}{2}\,\boldsymbol{.}\,\mathbf{n} - \frac{\gamma(u, v, \mathbf{n})}{2}\,(v - u)$$
- $\gamma(u, v, \mathbf{n}) = \max\left(\left|\mathbf{F}'(u)\,\boldsymbol{.}\,\mathbf{n}\right|, \left|\mathbf{F}'(v)\,\boldsymbol{.}\,\mathbf{n}\right|\right)$ Local Lax-Friedrichs

Subcell resolution of DG scheme

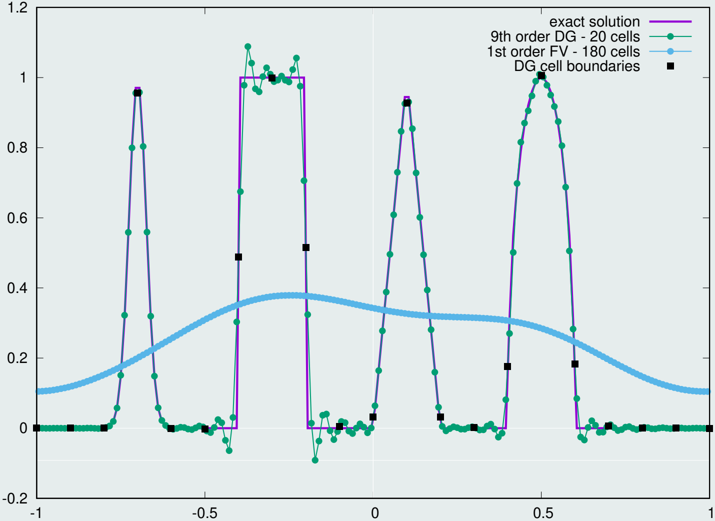

Figure : Linear advection of composite signal after 4 periods

Subcell resolution of DG scheme

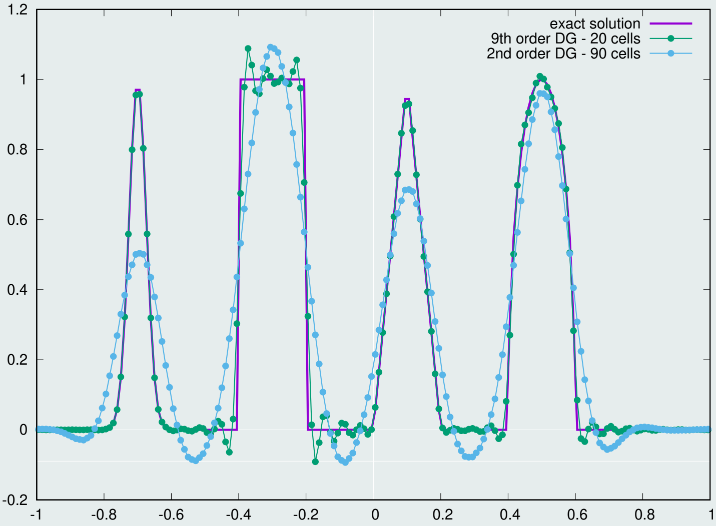

Figure : Linear advection of composite signal after 4 periods

Gibbs phenomenon

- High-order schemes leads to spurious oscillations near discontinuities
- Leads potentially to nonlinear instability, non-admissible solution, crash
- Vast literature of how prevent this phenomenon to happen:

$\Longrightarrow$ *a priori* and ***a posteriori*** limitations

A priori limitation

- Artificial viscosity
- Slope/moment/hierarchical limiter
- ENO/WENO limiter

A posteriori limitation

- MOOD ("Multi-dimensional Optimal Order Detection")
- Subcell finite volume limitation
- **Subcell limitation through flux reconstruction**

F. VILAR, *A Posteriori Correction of High-Order DG Scheme through Subcell Finite Volume Formulation and Flux Reconstruction.* JCP, 2018.

Admissible numerical solution

- Maximum principle / positivity preserving
- Prevent the code from crashing (for instance avoiding NaN)
- **Ensure the conservation of the scheme**

Spurious oscillations

- Discrete maximum principle
- Relaxing condition for smooth extrema

Accuracy

- Retain as much as possible the subcell resolution of the DG scheme
- Minimize the number of subcell solutions to recompute

Modify locally, at the subcell level, the numerical solution without impacting the solution elsewhere in the cell

1 Introduction

2 DG as a subcell finite volume

3 *A posteriori* subcell correction

4 Numerical results

5 Conclusion

DG as a subcell finite volume

- Rewrite DG scheme as a specific finite volume scheme on subcells
- Exhibit the corresponding subcell numerical fluxes: **reconstructed flux**

Cell subdivision into N_k subcells

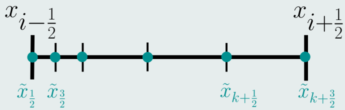

Figure : Example of a subdivision for a $\mathbb{P}^k$ DG scheme in 1D

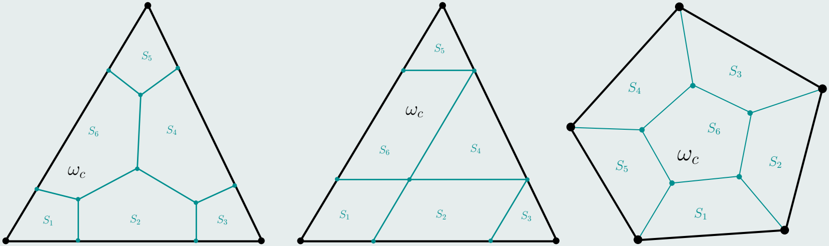

Figure : Examples of subdivision for a $\mathbb{P}^2$ DG scheme in 2D

DG schemes through residuals

- $$\sum_{m=1}^{N_k} \frac{\mathrm{d}\, u_m^c}{\mathrm{d}t} \int_{\omega_c} \sigma_m \, \sigma_p \, \mathrm{d}V = \int_{\omega_c} \mathbf{F}(u_h^c) \,\boldsymbol{.}\, \nabla \sigma_p \, \mathrm{d}V - \int_{\partial \omega_c} \sigma_p \, \mathcal{F}_n \, \mathrm{d}S, \qquad \forall\, p \in [\![1, N_k]\!]$$

$$\Longrightarrow \qquad \boxed{M_c \, \frac{\mathrm{d}\, U_c}{\mathrm{d}t} = \Phi_c}$$

- $(U_c)_m = u_m^c$ — Solution moments
- $(M_c)_{mp} = \int_{\omega_c} \sigma_m \, \sigma_p \, \mathrm{d}V$ — Mass matrix
- $(\Phi_c)_m = \int_{\omega_c} \mathbf{F}(u_h^c) \,\boldsymbol{.}\, \nabla \sigma_m \, \mathrm{d}V - \int_{\partial \omega_c} \sigma_m \, \mathcal{F}_n \, \mathrm{d}S$ — DG residuals

Subdivision and definition

- ω_c is subdivided into N_k subcells S_m^c
- Let us define $\overline{\psi}_m^c = \frac{1}{|S_m^c|} \int_{S_m^c} \psi \, \mathrm{d}V$ the subcell mean value

Submean values

- $$\int_{S_m^c} \frac{\partial u_h^c}{\partial t}\,\mathrm{d}V = |S_m^c|\,\frac{\mathrm{d}\,\overline{u}_m^c}{\mathrm{d}t}$$
- $$\frac{\mathrm{d}\,\overline{u}_m^c}{\mathrm{d}t} = \frac{1}{|S_m^c|}\sum_{q=1}^{N_k}\frac{\mathrm{d}\,u_q^c}{\mathrm{d}t}\int_{S_m^c}\sigma_q\,\mathrm{d}V$$

$$\Longrightarrow \boxed{\frac{\mathrm{d}\,\overline{U}_c}{\mathrm{d}t} = P_c\,\frac{\mathrm{d}\,U_c}{\mathrm{d}t}}$$

- $(\overline{U}_c)_m = \overline{u}_m^c$ — Submean values
- $(P_c)_{mp} = \dfrac{1}{|S_m^c|}\displaystyle\int_{S_m^c}\sigma_p\,\mathrm{d}V$ — Projection matrix

$$\Longrightarrow \boxed{\frac{\mathrm{d}\,\overline{U}_c}{\mathrm{d}t} = P_c\,M_c^{-1}\,\Phi_c}$$

Subcell Finite Volume: reconstructed fluxes

- Let us introduce the reconstructed fluxes such that

$$\boxed{\frac{\mathrm{d}\,\overline{u}_m^c}{\mathrm{d}t} = -\frac{1}{|S_m^c|}\int_{\partial S_m^c} \widehat{F_n}\,\mathrm{d}S}$$

- We impose that on the boundary of cell ω_c

$$\boxed{\widehat{F_n}_{|\partial\omega_c} = \mathcal{F}_n}$$

- $\displaystyle \frac{\mathrm{d}\,\overline{u}_m^c}{\mathrm{d}t} = -\frac{1}{|S_m^c|}\left(\sum_{f_{qq'}\in f_m^c}\int_{f_{qq'}} \widehat{F_n}\,\mathrm{d}S + \int_{\partial S_m^c\cap\partial\omega_c} \mathcal{F}_n\,\mathrm{d}S\right)$
- f_m^c Set of faces in $\partial S_m^c \setminus \partial\omega_c$
- $\displaystyle \int_{f_{qq'}} \widehat{F_n}\,\mathrm{d}S = \varepsilon_{qq'}\,\widehat{F_{qq'}}$
- $\varepsilon_{qq'}$ Sign function depending on the orientation of face $f_{qq'}$

Subcell Finite Volume: reconstructed fluxes

- $$\varepsilon_{qq'} = \begin{cases} 1 & \text{if the face } f_{qq'} \text{ is direct} \\ -1 & \text{if the edge } f_{qq'} \text{ is indirect} \\ 0 & \text{if } f_{qq'} \notin f_c = \bigcup_{m=1}^{N_k} f_m^c \end{cases}$$
- Let $\widehat{F_c}$ be the vector containing all the interior faces reconstructed fluxes
- The subcell mean values governing equations yield the following system

$$\boxed{-A_c\,\widehat{F_c} = D_c\,\frac{\mathrm{d}\,\overline{U}_c}{\mathrm{d}t} + B_c}$$

- $(A_c)_{qq'} = \varepsilon_{qq'}$ — Adjacency matrix
- $D_c = \operatorname{diag}\left(|S_1^c|, \ldots, |S_{N_k}^c|\right)$ — Subcells volume matrix
- $(B_c)_m = \int_{\partial S_m^c \cap \partial \omega_c} \mathcal{F}_n \,\mathrm{d}S$ — Cell boundary contribution

Subcell Finite Volume: reconstructed fluxes

- Introducing $Q_c = D_c \, P_c$ such that $(Q_c)_{mp} = \displaystyle\int_{S_m^c} \sigma_p \, \mathrm{d}V$, one finally gets

$$\boxed{-A_c \, \widehat{F_c} = Q_c \, M_c^{-1} \, \Phi_c + B_c}$$

Graph Laplacian technique

- $A_c \in \mathcal{M}_{N_k \times N_F}$ with $N_F = \mathrm{Card}(\mathcal{S}_c)$ the number of interior faces
- $A_c^{\mathrm{t}} \, \mathbf{1} = \mathbf{0}$ where $\mathbf{1} = (1, \dots, 1)^{\mathrm{t}} \in \mathbb{R}^{N_k}$

R. Abgrall, *Some Remarks about Conservation for Residual Distribution Schemes.* Methods Appl. Math., 18:327-351, 2018.

- Let $\mathcal{L}_c^{-1}$ be the inverse of $L_c = A_c \, A_c^{\mathrm{t}}$ on the orthogonal of its kernel

$$\boxed{\mathcal{L}_c^{-1} = (L_c + \lambda \, \Pi)^{-1} - \frac{1}{\lambda} \, \Pi} \qquad \forall \lambda \neq 0$$

- $\Pi = \frac{1}{N_k} \, (\mathbf{1} \otimes \mathbf{1}) \in \mathcal{M}_{N_k}$

Graph Laplacian technique

- Finally, we obtain the following definition of the reconstructed fluxes

$$\boxed{\widehat{F_c} = -A_c^{\mathrm{t}}\,\mathcal{L}_c^{-1}\left(Q_c\,M_c^{-1}\,\Phi_c + B_c\right)}$$

remark

- The only terms depending on the time are Φ_c and B_c

Back to the DG scheme

- The polynomial solution is defined through reconstructed fluxes as follows

$$\boxed{\frac{\mathrm{d}\,U_c}{\mathrm{d}t} = -Q_c^{-1}\left(A_c\,\widehat{F_c} + B_c\right)}$$

Question

- Is the reconstructed flux $\widehat{F_c}$ close to the interior flux $\boldsymbol{F}(u_h^c)$?

Local variational formulation

- $\displaystyle\int_{\omega_c} \frac{\partial u_h^c}{\partial t}\,\psi\,\mathrm{d}V = \int_{\omega_c} \mathbf{F}(u_h^c)\,\boldsymbol{.}\,\nabla\psi\,\mathrm{d}V - \int_{\partial\omega_c} \psi\,\mathcal{F}_n\,\mathrm{d}S, \qquad \forall\,\psi \in \mathbb{P}^k(\omega_c)$
- Substitute $\boldsymbol{F}(u_h^c)$ with $\boldsymbol{F}_h^c \in \left(\mathbb{P}^{k+1}(\omega_c)\right)^2$ (collocated or L_2 projection)
- $\displaystyle\int_{\omega_c} \frac{\partial u_h^c}{\partial t}\,\psi\,\mathrm{d}V = -\int_{\omega_c} \psi\,\nabla\,\boldsymbol{.}\,\boldsymbol{F}_h^c\,\mathrm{d}V + \int_{\partial\omega_c} \psi\,\left(\boldsymbol{F}_h^c\,\boldsymbol{.}\,\boldsymbol{n} - \mathcal{F}_n\right)\,\mathrm{d}S, \quad \forall\,\psi \in \mathbb{P}^k(\omega_c)$

Subresolution basis functions

- Let us introduce the N_k basis functions $\{\phi_m\}_m$ such that $\forall\,\psi \in \mathbb{P}^k(\omega_c)$

$$\int_{\omega_c} \phi_m\,\psi\,\mathrm{d}V = \int_{S_m^c} \psi\,\mathrm{d}V, \qquad \forall\, m = 1, \ldots, N_k,$$

- $\displaystyle\sum_{m=1}^{N_k} \phi_m(\boldsymbol{x}) = 1$

These particular functions can be seen as the L_2 projection of the indicator functions $\mathbb{1}_m(\boldsymbol{x})$ onto $\mathbb{P}^k(\omega_c)$

Subcell finite volume scheme

- $$\int_{\omega_c} \frac{\partial u_h^c}{\partial t}\,\phi_m \,\mathrm{d}V = -\int_{\omega_c} \phi_m \nabla \cdot \boldsymbol{F}_h^c \,\mathrm{d}V + \int_{\partial\omega_c} \phi_m \,\left(\boldsymbol{F}_h^c \cdot \boldsymbol{n} - \mathcal{F}_n\right)\,\mathrm{d}S$$
- $$|S_m^c|\,\frac{\mathrm{d}\,\overline{u}_m^c}{\mathrm{d}t} = -\int_{S_m^c} \nabla \cdot \boldsymbol{F}_h^c \,\mathrm{d}V + \int_{\partial\omega_c} \phi_m \,\left(\boldsymbol{F}_h^c \cdot \boldsymbol{n} - \mathcal{F}_n\right)\,\mathrm{d}S$$
- $$\frac{\mathrm{d}\,\overline{u}_m^c}{\mathrm{d}t} = -\frac{1}{|S_m^c|}\left(\int_{\partial S_m^c} \boldsymbol{F}_h^c \cdot \boldsymbol{n}\,\mathrm{d}S - \int_{\partial\omega_c} \phi_m \,\left(\boldsymbol{F}_h^c \cdot \boldsymbol{n} - \mathcal{F}_n\right)\,\mathrm{d}S\right)$$
- $$\frac{\mathrm{d}\,\overline{u}_m^c}{\mathrm{d}t} = -\frac{1}{|S_m^c|}\int_{\partial S_m^c} \widehat{F}_n \,\mathrm{d}S$$ Subcell finite volume

Reconstructed Fluxes

- Finally, we get that

$$\boxed{\int_{\partial S_m^c} \widehat{F}_n \,\mathrm{d}S = \int_{\partial S_m^c} \boldsymbol{F}_h^c \cdot \boldsymbol{n}\,\mathrm{d}S - \int_{\partial\omega_c} \phi_m \,\left(\boldsymbol{F}_h^c \cdot \boldsymbol{n} - \mathcal{F}_n\right)\,\mathrm{d}S}$$

Reconstructed fluxes

- As we impose that $\widehat{F_n}_{|\partial\omega_c} = \mathcal{F}_n$, this last expression rewrites

$$\int_{\partial S_m^c \setminus \partial\omega_c} \widehat{F_n}\,\mathrm{d}S = \int_{\partial S_m^c \setminus \partial\omega_c} \boldsymbol{F}_h^c \,.\, \boldsymbol{n}\,\mathrm{d}S - \int_{\partial\omega_c} \widetilde{\phi_m}\,\left(\boldsymbol{F}_h^c \,.\, \boldsymbol{n} - \mathcal{F}_n\right)\,\mathrm{d}S$$

- $\widetilde{\phi_m} = \begin{cases} \phi_m & \text{if } \boldsymbol{x} \in \partial\omega_c \setminus \partial S_m^c \\ \phi_m - 1 & \text{if } \boldsymbol{x} \in \partial\omega_c \bigcap \partial S_m^c \end{cases}$

- $\displaystyle\int_{f_{qq'}} \widehat{F_n}\,\mathrm{d}S = \varepsilon_{qq'}\,\widehat{F_{qq'}}$ and $\displaystyle\int_{f_{qq'}} \boldsymbol{F}_h^c \,.\, \boldsymbol{n}\,\mathrm{d}S = \varepsilon_{qq'}\,F_{qq'}$

- Then, if F_c is the vector containing all the interior faces fluxes, one gets

$$\boxed{A_c\,\widehat{F_c} = A_c\,F_c - G_c}$$

- $(G_c)_m = \displaystyle\int_{\partial\omega_c} \widetilde{\phi_m}\,\left(\boldsymbol{F}_h^c \,.\, \boldsymbol{n} - \mathcal{F}_n\right)\,\mathrm{d}S$ Boundary contribution

Reconstructed fluxes through interior fluxes

- Making use of the same graph Laplacian technique, we finally obtain

$$\boxed{\widehat{F_c} = F_c - A_c^{\mathrm{t}} \mathcal{L}_c^{-1} G_c}$$

- We can rewrite this expression as

$$\widehat{F_c} = F_c - E\left(\boldsymbol{F}_h^c \,.\, \boldsymbol{n} - \mathcal{F}_n\right)$$

where $E(.)$ is a correction function taking into account the jump between the polynomial flux and the numerical flux on the cell boundary

Remark

- Different choice in the correction function $E(.)$ leads to different scheme
- For instance, $E = 0$ leads to the spectral volume scheme of Z.J. Wang

Reconstructed flux in the 1D case

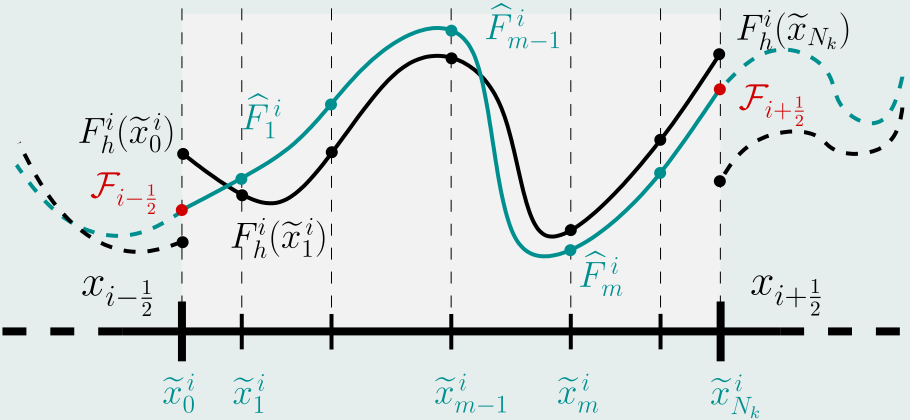

Figure : Polynomial interior flux and reconstructed flux

1. Introduction
2. DG as a subcell finite volume
3. *A posteriori* subcell correction
4. Numerical results
5. Conclusion

RKDG scheme

- SSP Runge-Kutta: convex combinations of first-order forward Euler
- For sake of clarity, we focus on forward Euler time stepping

Projection on subcells of RKDG solution

- $u_h^{c,n}(x) = \sum_{m=1}^{N_k} u_m^{c,n}\, \sigma_m(x)$
- $u_h^{c,n}$ is uiquely defined by its N_k submean values $\overline{u}_m^{c,n}$
- Recalling the definition of the projection matrix $(P_c)_{mp} = \dfrac{1}{|S_m^c|} \displaystyle\int_{S_m^c} \sigma_p \,\mathrm{d}V,$

$$\Longrightarrow \qquad P_c \begin{pmatrix} u_1^{c,n} \\ \vdots \\ u_{N_k}^{c,n} \end{pmatrix} = \begin{pmatrix} \overline{u}_1^{c,n} \\ \vdots \\ \overline{u}_{N_k}^{c,n} \end{pmatrix}$$

Set up

- We assume that, for each cell, the $\{\overline{u}_m^{c,n}\}_m$ are admissible
- Compute a candidate solution u_h^{n+1} from u_h^n through uncorrected DG
- For each subcell, check if the submean values $\{\overline{u}_m^{c,n+1}\}_m$ are ok

Physical admissibility detection (PAD)

- Check if $\overline{u}_m^{c,n+1}$ lies in an convex physical admissible set (maximum principle for SCL, positivity of the pressure and density for Euler, . . .)
- Check if there is any *NaN* values

Numerical admissibility detection (NAD)

- Discrete maximum principle DMP on submean values:

$$\min_{\substack{p \in [\![1, N_k]\!] \\ v \in \mathcal{V}(\omega_c)}} (\overline{u}_p^{c,n}, \overline{u}_p^{v,n}) \leq \overline{u}_m^{c,n+1} \leq \max_{\substack{p \in [\![1, N_k]\!] \\ v \in \mathcal{V}(\omega_c)}} (\overline{u}_p^{c,n}, \overline{u}_p^{v,n})$$

- This criterion needs to be relaxed to preserve smooth extrema

Corrected reconstructed flux

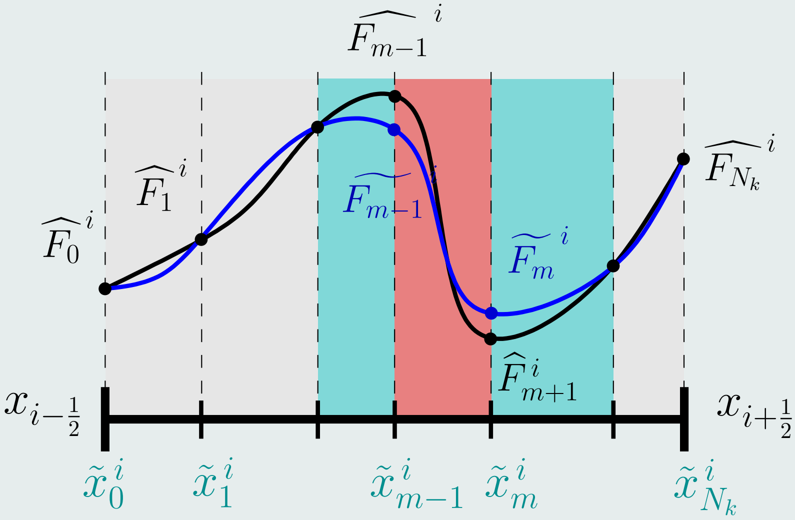

Figure : Correction of the reconstructed flux

Corrected reconstructed flux

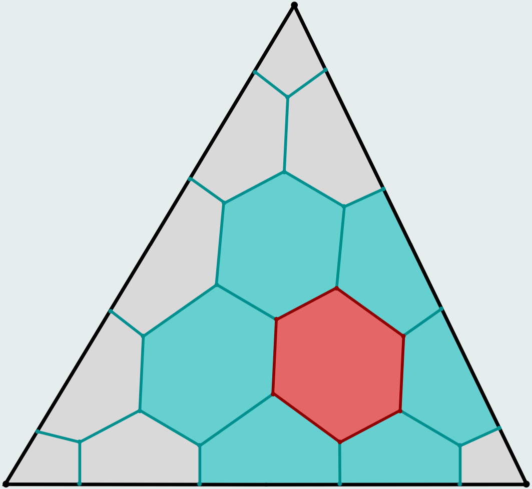

Figure : Correction of the reconstructed flux

Flowchart

1. Compute the uncorrected DG candidate solution $u_h^{c,n+1}$
2. Project $u_h^{c,n+1}$ to get the submean values $\overline{u}_m^{c,n+1}$
3. Check $\overline{u}_m^{c,n+1}$ through the troubled zone detection plus relaxation
4. If $\overline{u}_m^{c,n+1}$ is admissible go further in time, otherwise modify the corresponding reconstructed flux values

$$\forall f_{mq} \in \partial S_m^c, \qquad \boxed{\widehat{F_{mq}} = \mathcal{F}\left(\overline{u}_m^{c,n}, \overline{u}_q^{c,n}, \boldsymbol{n}_{mq}\right)}$$

5. Through the corrected reconstructed flux, recompute the submean values for tagged subcells and their first neighbors
6. Return to 3

Conclusion

- The limitation only affects the DG solution at the subcell scale
- The corrected scheme is conservative at the subcell level
- In practice, few submean values need to be recomputed

1 Introduction

2 DG as a subcell finite volume

3 *A posteriori* subcell correction

4 Numerical results

5 Conclusion

Initial solution on $x \in [0, 1]$

- $u_0(x) = \sin(2\pi x)$
- Periodic boundary conditions

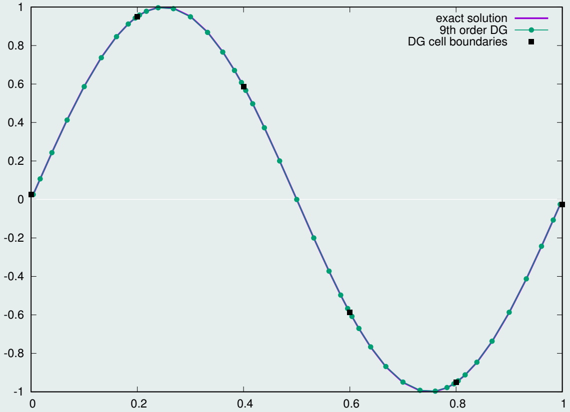

Figure : Linear advection with a 9th DG scheme and 5 cells after 1 period

Convergence rates

	L_1		L_2	
h	$E^h_{L_1}$	$q^h_{L_1}$	$E^h_{L_2}$	$q^h_{L_2}$
$\frac{1}{20}$	8.07E-11	9.00	8.97E-11	9.00
$\frac{1}{40}$	1.58E-13	9.00	1.75E-13	9.00
$\frac{1}{80}$	3.08E-16	-	3.42E-16	-

Table: Convergence rates for the linear advection case for a 9th order DG scheme

Linear advection of a square signal after 1 period

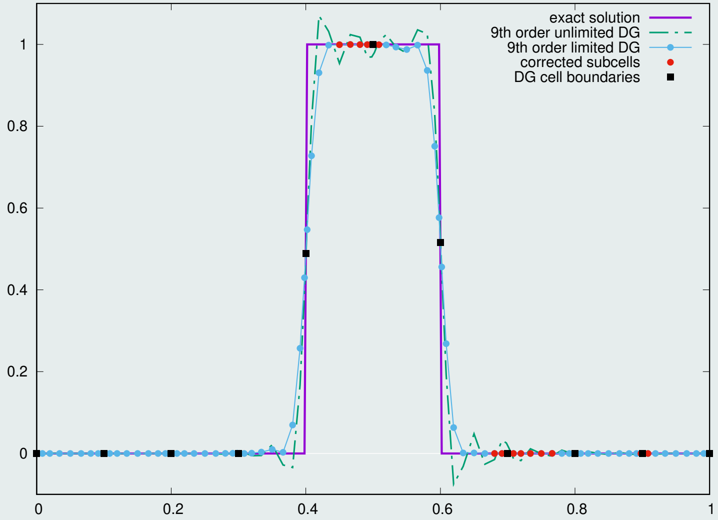

Figure : 9th order corrected and uncorrected DG solutions

Linear advection of a square signal after 10 periods

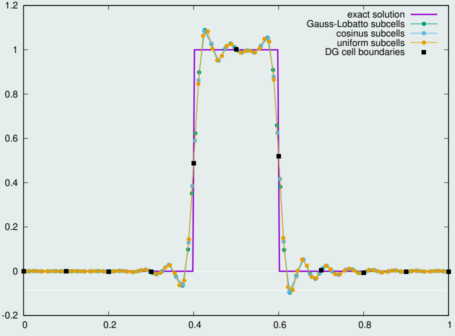

(a) Without correction

(b) With correction

Figure : Comparison between different cell subdivision

Linear advection of a square signal

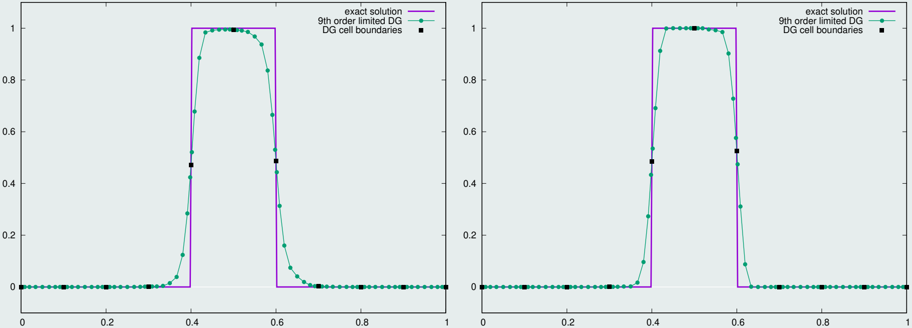

(a) 1st-order correction

(b) 2nd-order correction

Figure : Comparison between 1st and 2nd order correction for the SubNAD detection criterion

Linear advection of a composite signal after 4 periods

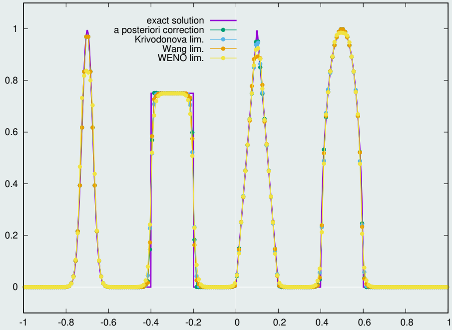

(a) 200 cells: cell mean values

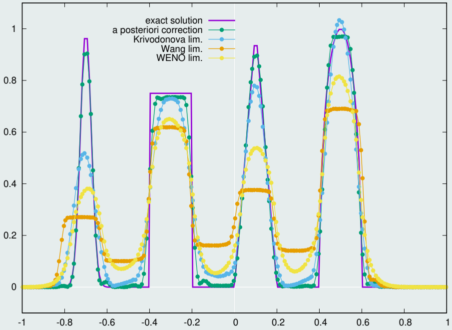

(b) 50 cells: subcell mean values

Figure : 4th order DG solutions provided different limitations

Linear advection of a composite signal after 4 periods

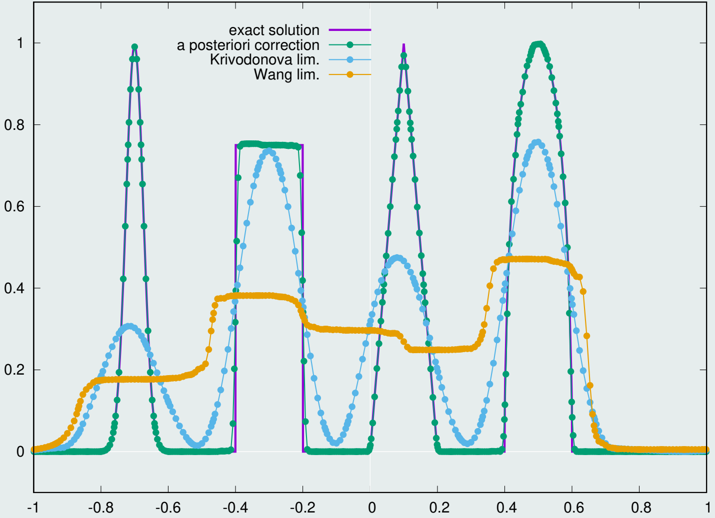

Figure : 9th order DG solutions provided different limitations on 30 cells

Burgers equation: $u_0(x) = \sin(2\pi\, x)$

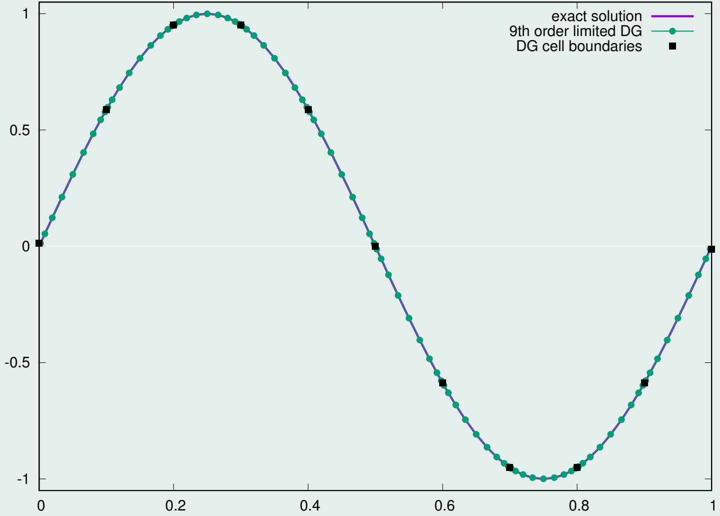

Figure : 9th order corrected DG on 10 cells for $t_f = 0.7$

Burgers equation: expansion and shock waves collision

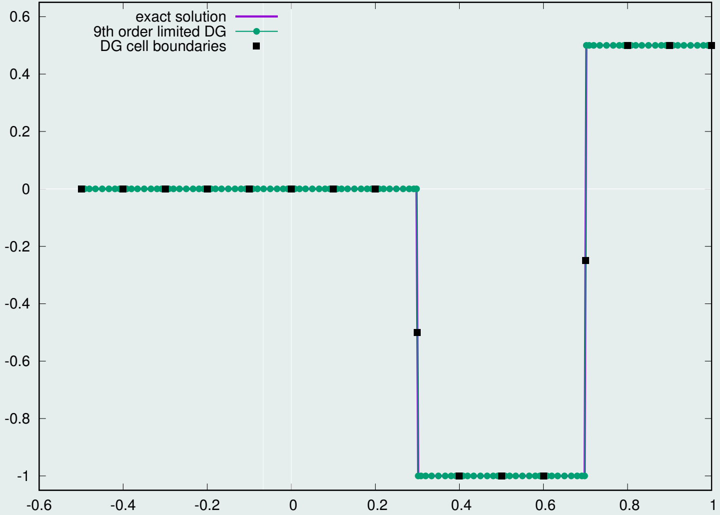

Figure : 9th order corrected DG on 15 cells for $t_f = 1.2$

Burgers equation: expansion and shock waves collision

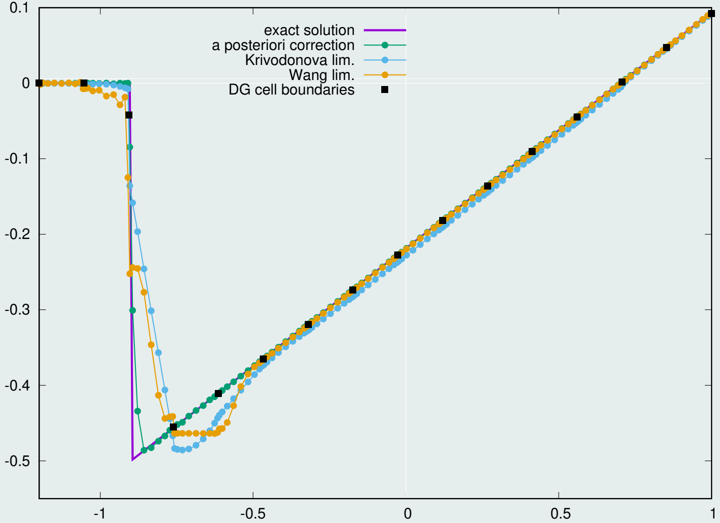

Figure : 9th order corrected DG on 15 cells provided different limitations

Buckley non-convex flux problem at time $t = 0.4$

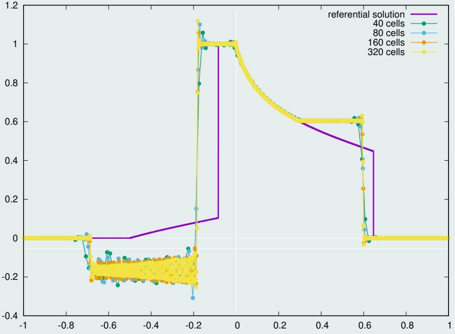

(a) Non-entropic behavior (b) Aliasing phenomenon

Figure : Uncorrected DG solution for the Buckley non-convex flux case

Buckley non-convex flux problem at time $t = 0.4$

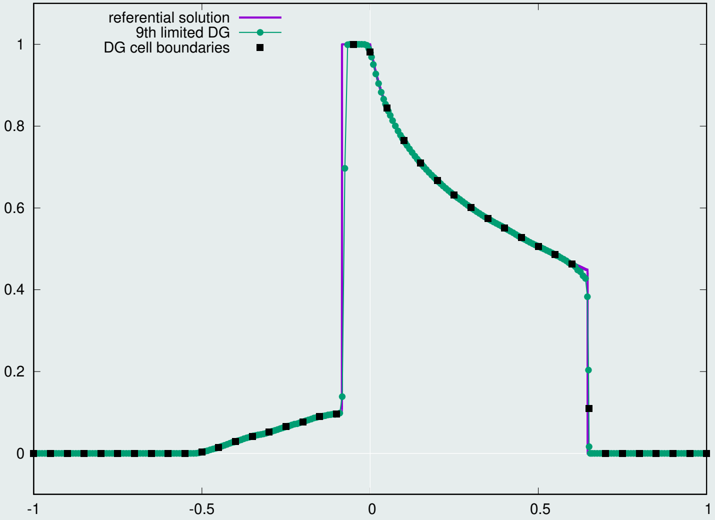

Figure : 9th order corrected DG solutions on 40 cells

Buckley non-convex flux problem at time $t = 0.4$

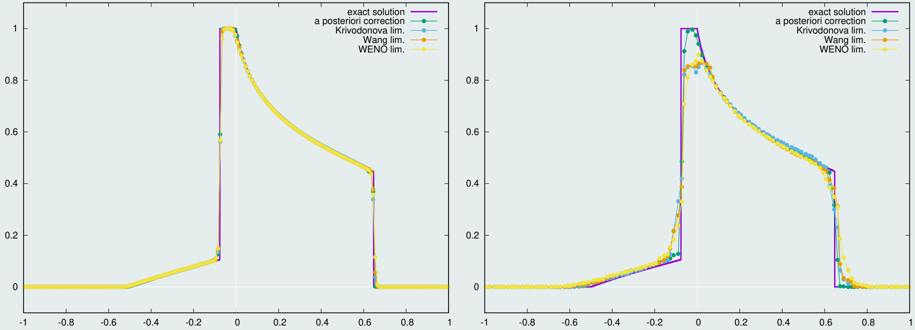

(a) 200 cells: cell mean values

(b) 30 cells: subcell mean values

Figure : 4th order DG solutions provided different limitations

Buckley non-convex flux problem at time $t = 0.4$

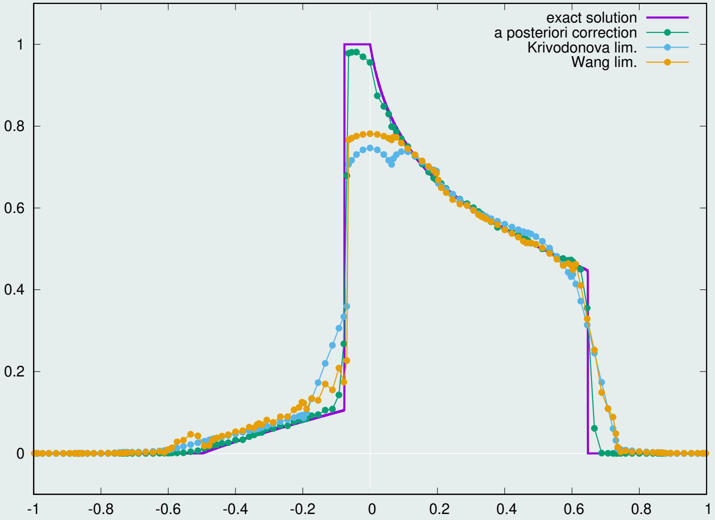

Figure : 9th order DG solutions provided different limitations on 15 cells

Initial solution on $x \in [0,1]$ for $\gamma = 3$

- $\rho_0(x) = 1 + 0.9999999\sin(\pi x), \quad u_0(x) = 0, \quad p_0(x) = (\rho_0(x))^\gamma$

$$\Longrightarrow \rho_0(-\tfrac{1}{2}) = 1.E-7 \quad \text{and} \quad p_0(-\tfrac{1}{2}) = 1.E-21$$

- Periodic boundary conditions

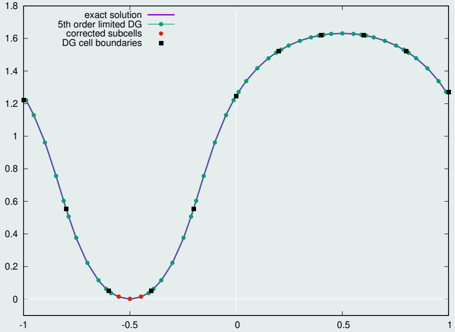

(a) Density

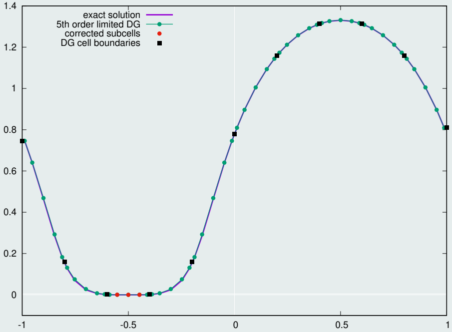

(b) Internal energy

Figure : 5th order corrected DG solution on 10 cells at $t = 0.1$

Convergence rates

	L_1		L_2		Average % of corrected subcells
h	$E_{L_1}^h$	$q_{L_1}^h$	$E_{L_2}^h$	$q_{L_2}^h$	
$\frac{1}{20}$	1.48E-5	4.35	2.02E-5	4.18	6.87 %
$\frac{1}{40}$	9.09E-7	4.88	1.38E-6	4.87	3.31 %
$\frac{1}{80}$	3.09E-8	4.95	4.73E-8	4.86	2.50 %
$\frac{1}{160}$	1.00E-9	-	1.63E-9	-	1.12 %

Table: Convergence rates on the pressure for the Euler equation for a 5th order DG

Sod shock tube problem

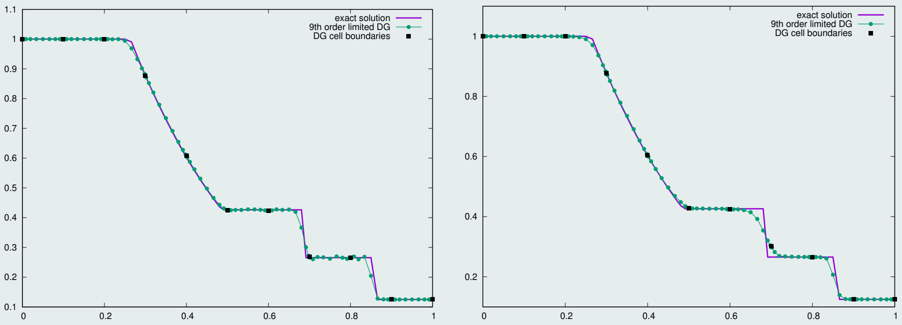

(a) NAD + 1st order correction (b) SubNAD + 2nd order correction

Figure : 9th order corrected DG on 10 cells

Sod shock tube problem

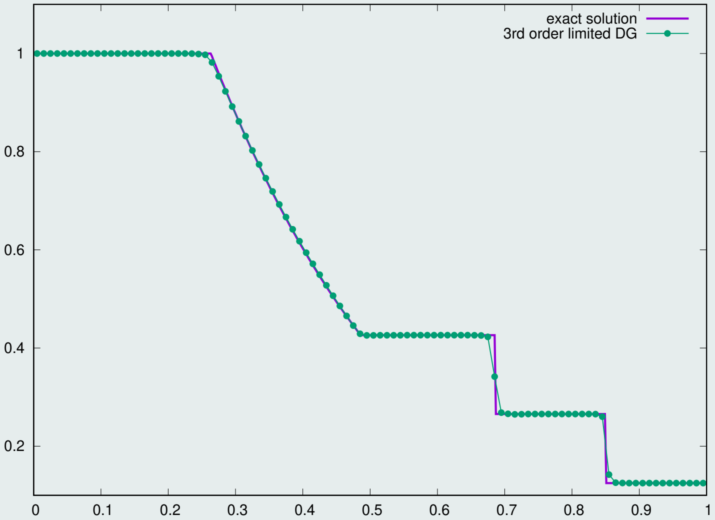

Figure : 3rd order DG solutions on 100 cells: cell mean values

Shock acoustic-wave interaction problem

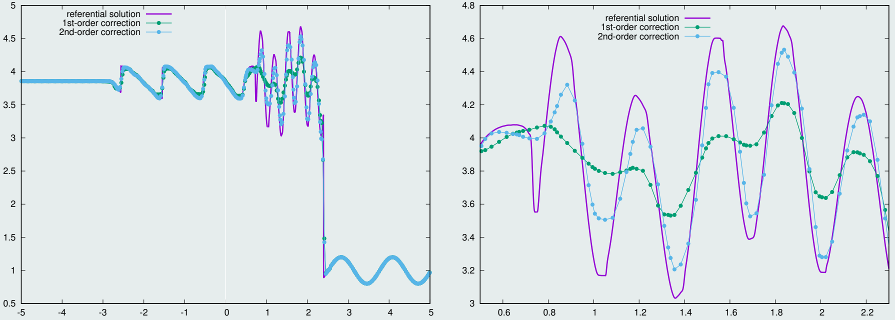

(a) Global view

(b) Zoom on $[0.5, 2.3]$

Figure : 7th order corrected DG on 50 cells: comparison between 1st and 2nd order corrections

Shock acoustic-wave interaction problem

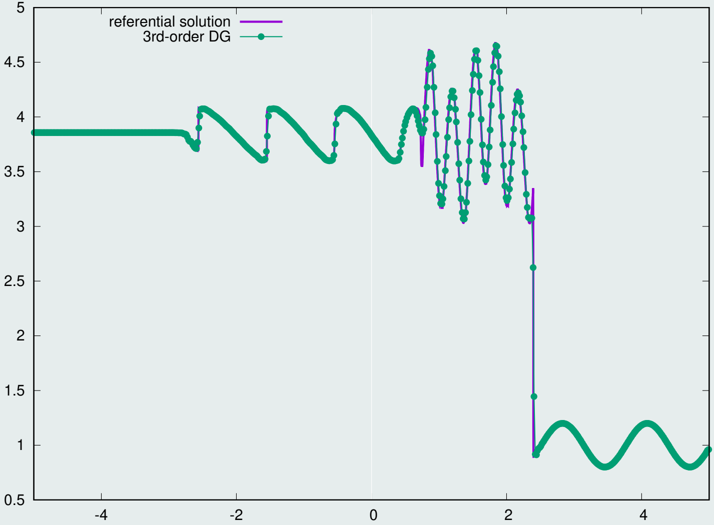

Figure : 3rd order corrected DG solutions on 200 cells: cell mean values

Blast waves interaction problem

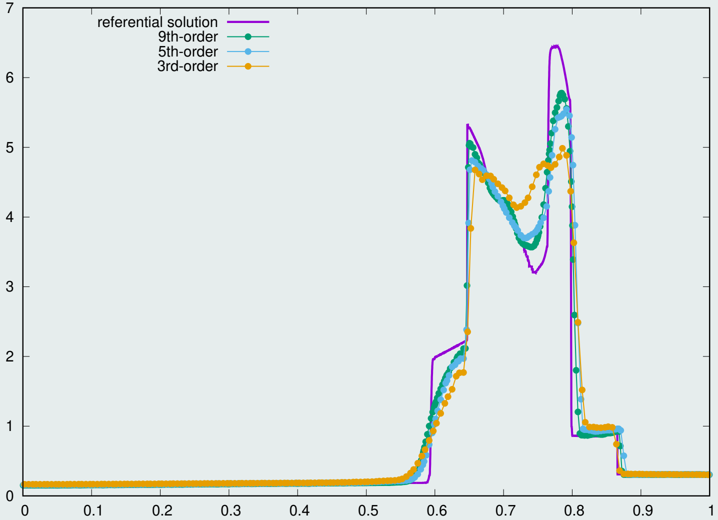

Figure : Corrected DG solution on 60 cells, from 3rd to 9th order

2D grid and subgrid

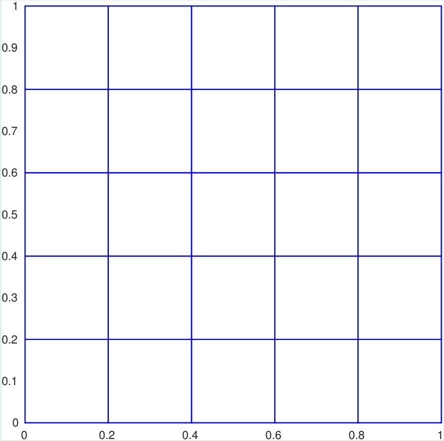

(a) Grid

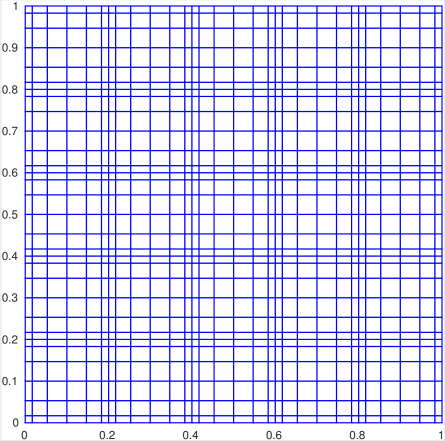

(b) Subgrid

Figure : 5x5 Cartesian grid and corresponding subgrid for a 6th order DG scheme

Initial solution on $(x, y) \in [0, 1]^2$

- $u_0(x, y) = \sin(2\pi(x + y))$
- Periodic boundary conditions

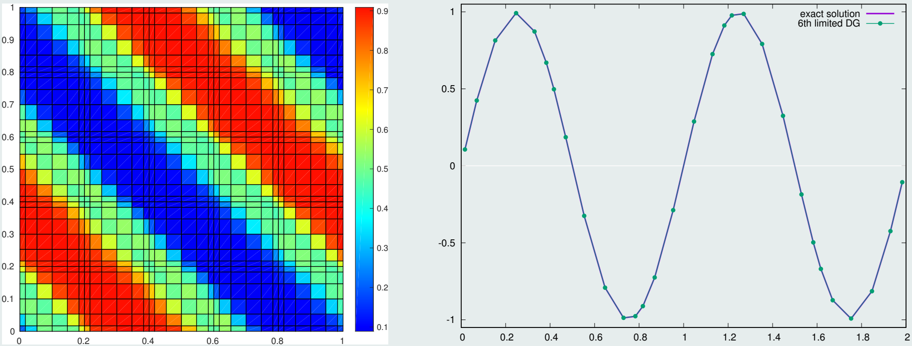

(a) Solution map (b) Solution profile

Figure : Linear advection with a 6th DG scheme and 5x5 grid after 1 period

Convergence rates

	L_1		L_2	
h	$E^h_{L_1}$	$q^h_{L_1}$	$E^h_{L_2}$	$q^h_{L_2}$
$\frac{1}{5}$	2.10E-6	6.23	2.86E-6	6.24
$\frac{1}{10}$	2.79E-8	6.00	3.77E-8	6.00
$\frac{1}{20}$	3.36E-10	-	5.91E-10	-

Table: Convergence rates for the linear advection case for a 6th order DG scheme

Rotation of a composite signal after 1 period

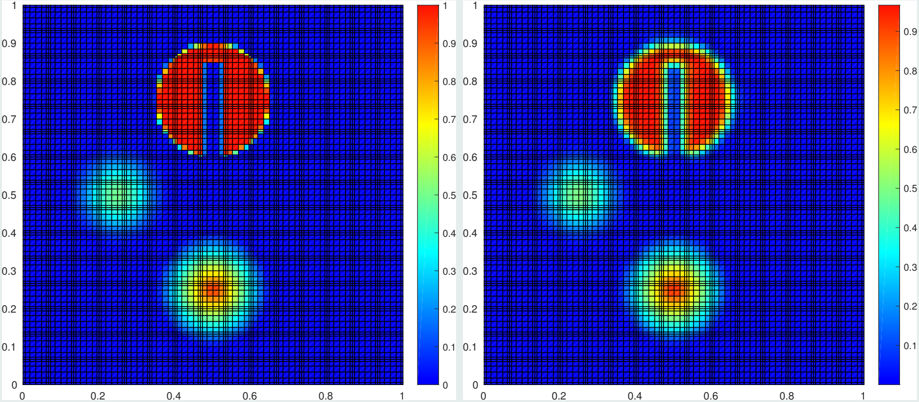

(a) Initial solution (b) Final solution

Figure : 6th order corrected DG on a 15x15 Cartesian mesh

Rotation of a composite signal after 1 period

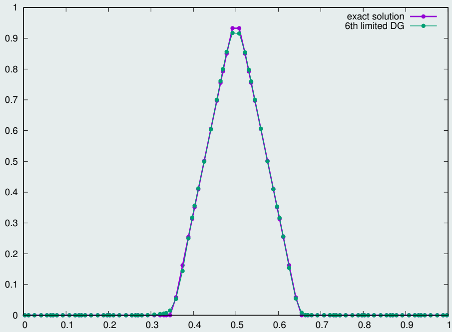

(a) Solution profile for $y = 0.25$

(b) Solution profile for $y = 0.75$

Figure : 6th order corrected DG on a 15x15 Cartesian mesh

Rotation of a composite signal after 1 period: $x = 0.25$

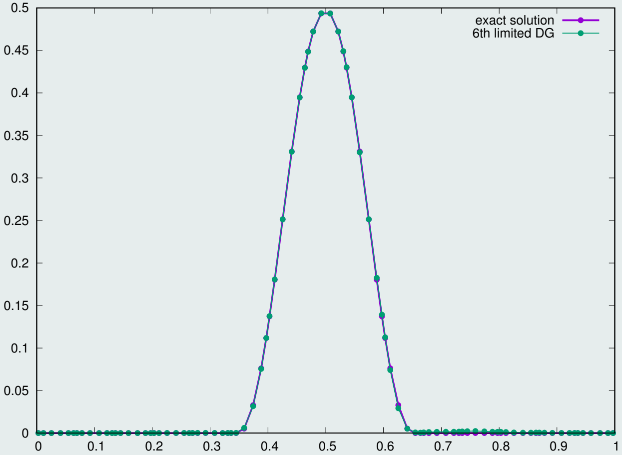

Figure : 6th order corrected DG on a 15x15 Cartesian mesh

Burgers equation with $u_0(x, y) = \sin(2\pi(x + y))$

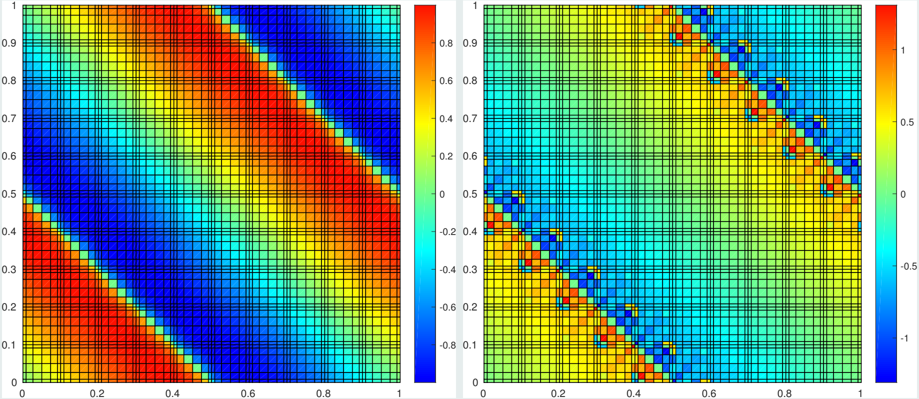

(a) Solution at $t = 0.007$ (b) Solution at $t = 0.25$

Figure : 6th order uncorrected DG on a 10x10 Cartesian mesh

Burgers equation with $u_0(x, y) = \sin(2\pi(x + y))$

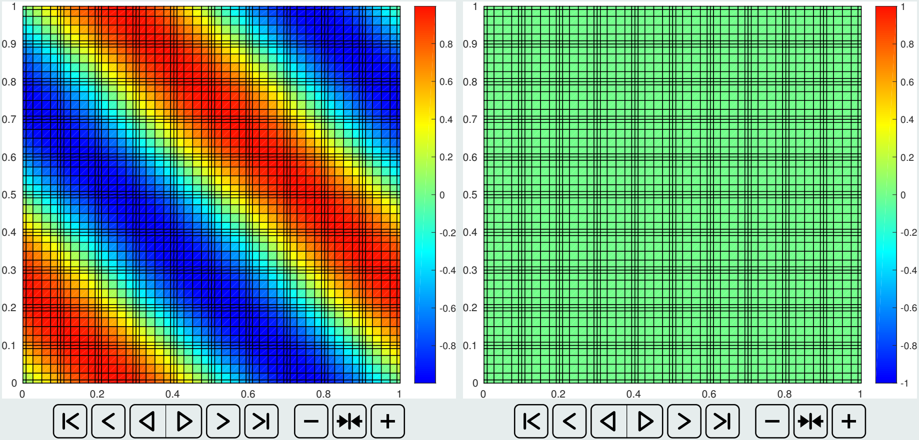

(a) Solution map (b) Detected subcells

Figure : 6th order corrected DG on a 10x10 Cartesian mesh until $t = 0.5$

Burgers equation with $u_0(x,y) = \sin(2\pi\,(x+y))$ at $t = 0.5$

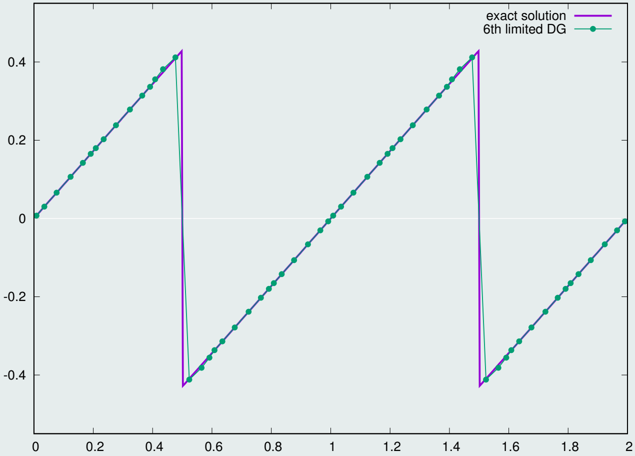

Figure : 6th order corrected DG solution profile on a 10x10 Cartesian mesh

Burgers equation with composite signal

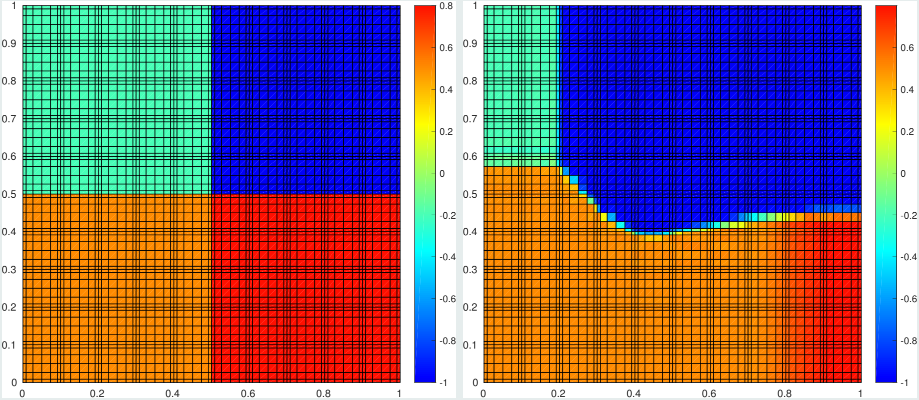

(a) Initial solution

(b) Solution at $t = 0.5$

Figure : 6th order corrected DG on a 10x10 Cartesian mesh

Kurganov, Petrova, Popov (KPP) non-convex flux problem

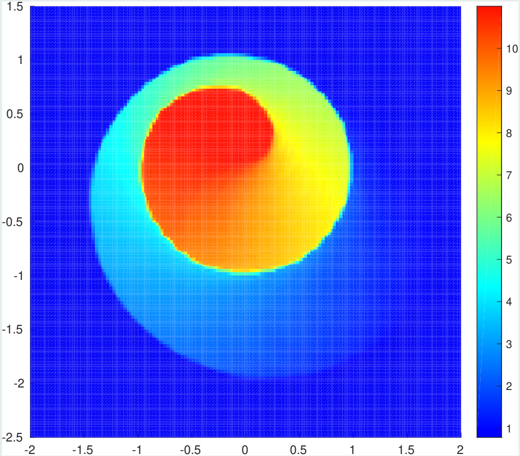

Figure : 6th order corrected DG solution on a 30x30 Cartesian mesh

Ongoing work

- Extension to unstructured grids (with R. Abgrall): **numerical results**
- DoF based adaptive DG scheme through subcell finite volume formulation (with R. Loubère, S. Clain and G. Gassner)
- Maximum principle preserving DG scheme through subcell FCT reconstructed flux

Published paper

F. VILAR, *A Posteriori Correction of High-Order DG Scheme through Subcell Finite Volume Formulation and Flux Reconstruction.* JCP, 387:245-279, 2018.

Linear advection of a square signal

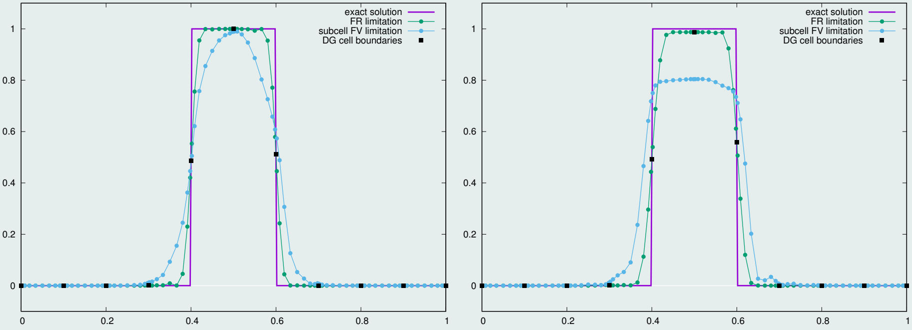

(a) After 1 period (b) After 50 periods

Figure : Comparison between subcell FV limitation and the present correction

Linear advection of a composite signal after 4 periods

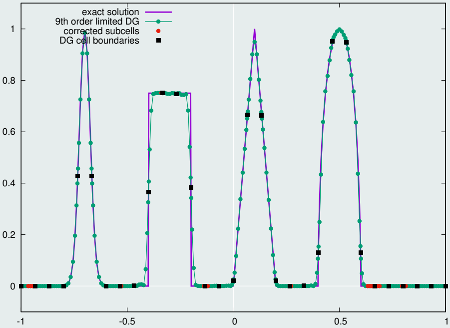

(a) NAD and 1st-order correction

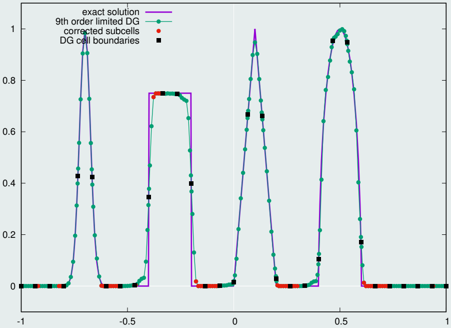

(b) SubNAD and 2nd-order correction

Figure : 9th order corrected DG on 30 cells